A benzothiazole-based new fluorogenic ratiometric chemosensor for CN^- and its real time application in environmental water samples and living cells

Dhanapal Jothi[a], Sathishkumar Munusamy[b], Selin Manojkumar[a], Saravanan Enbanathan[a] and Sathiyanarayanan KulathuIyer[a]*

[a]Department of Chemistry, School of Advanced Sciences and Vellore Institute of Technology, Vellore-632014, India. *E-mail: sathiya_kuna@hotmail.com

[b]Institute of chemical biology and nanomedicine, State key laboratory of chemo/Bio-sensing and Chemometrics, College of Chemistry and Chemical Engineering, Hunan University, Changsha 410082, P.R.China. E-mail: pra3sat@gmail.com

Table of contents

Fig S1 ^{1}H NMR spectra of **BID** **S3**

Fig S2 ^{13}C NMR spectra of **BID** **S3**

Fig S3 HRMS spectra of **BID** and **BID +CN^-** **S4-S5**

Fig S4 UV-vis absorption and photoluminescence properties of **BID** in toluene solvent; excitation wavelength is 408nm. **S5**

Fig S5 The Lippert-Mattaga plot for **BID** showing the Stokes shift versus orientation polarizability. **S6**

Fig S6 Linear plot of **BID + CN^-**. The calculated limit of detection of 5.97 nM. **S6**

Fig S7 The effect of salt **(a, b)** on the normalized fluorescence intensity of **BID** and **BID+CN^-.** **S7**

Fig S8 IR spectra of **BID** and **BID +CN^-** **S7**

Fig S9 The entire geometry optimizations structure of **BID** and **BID+CN^-** determined by DFT/B3LYP methods **S8**

Table S1 Oscillator strengths of important transitions for the BID and BID + CN^- determined by DFT/B3LYP methods. **S8**

Fig S10 Quantitative calibration plot results for BID and incremental addition of CN^- (2-10 μM) for BID-CN^- samples in D_2O. **S9**

Table S2 Results of CN^- readings in DMSO samples**.** **S9**

Fig S11 Cytotoxicity assay of sensor probe **BID** **S10**

Table S3 Comparison of LOD of CN^- detection reported in recent papers. **S10-S11**

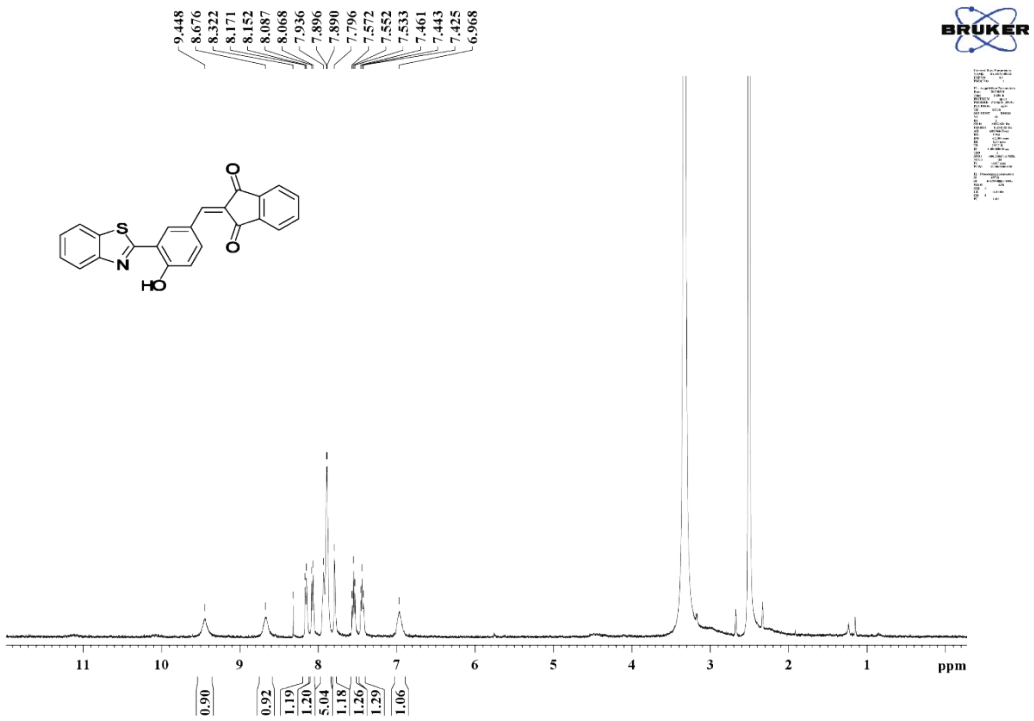

Fig S1 ^{1}H NMR spectra of **BID.**

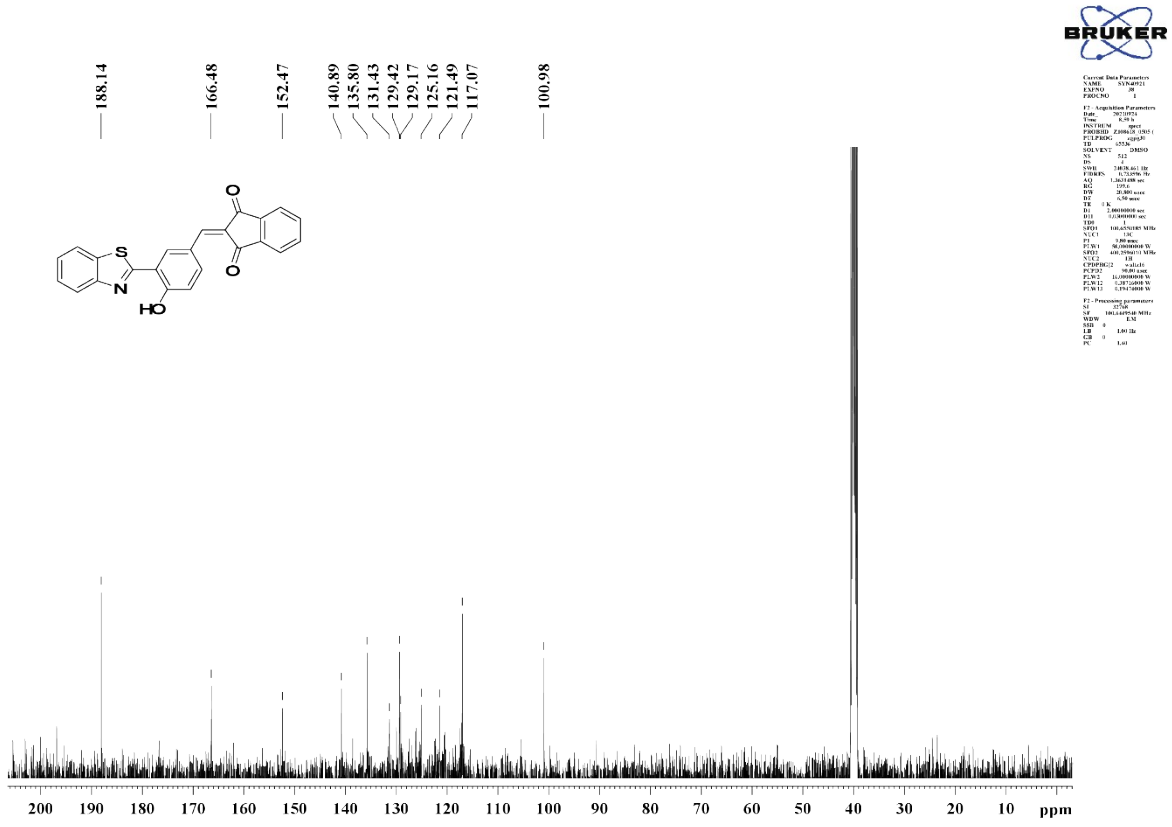

Fig S2 ^{13}C NMR spectra of **BID.**

Sample Name	060319-38-EXT-DK	**Position**	P2-D5	**Instrument Name**	Instrument 1
User Name		**Inj Vol**	5	**InjPosition**	
Sample Type	Sample	**IRM Calibration Status**	Success	**Data Filename**	OPSDSABB.d
ACQ Method	Direct Infusion_HPLC.m	**Comment**		**Acquired Time**	06-03-2019 11:45:56 (UTC+05:30)

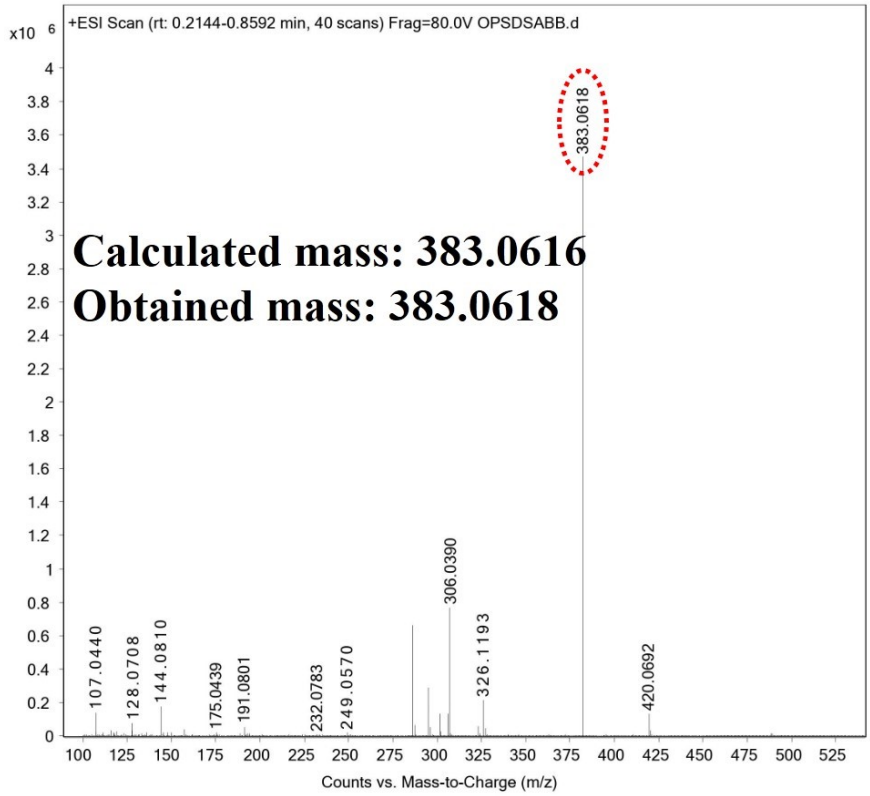

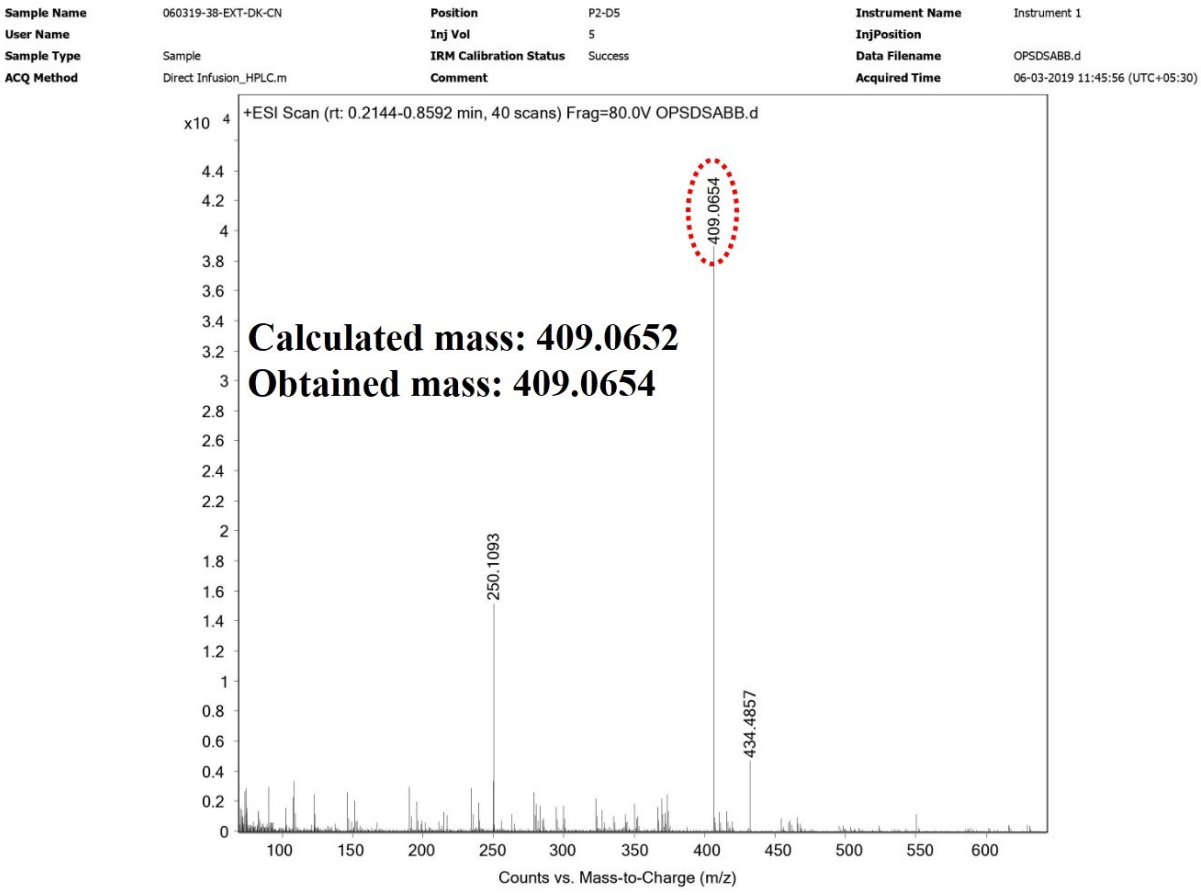

Fig S3 HRMS spectra of **BID** and **BID +CN$^-$.**

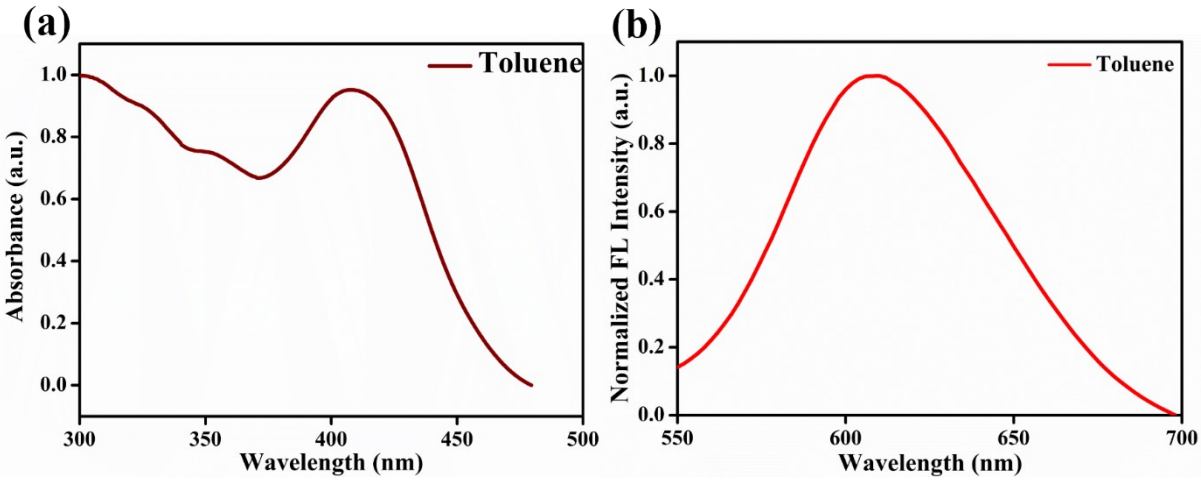

Fig S4 UV-vis absorption and photoluminescence properties of **BID** in toluene solvent excitation wavelength is 408nm.

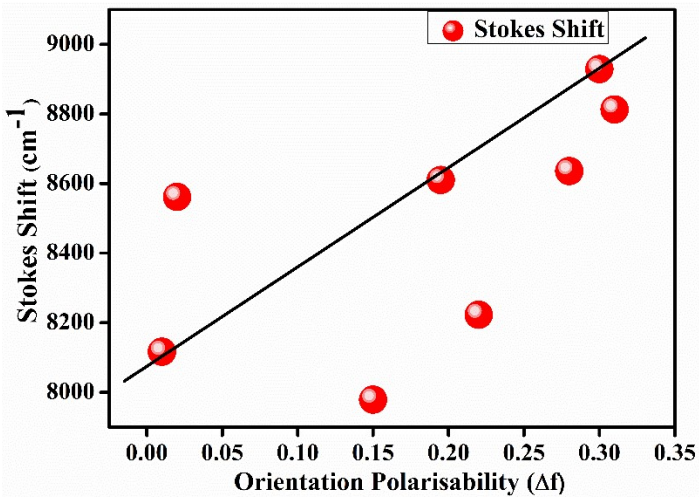

Fig S5 The Lippert-Mattaga plot of **BID** showing the Stokes shift versus orientation polarizability**.**

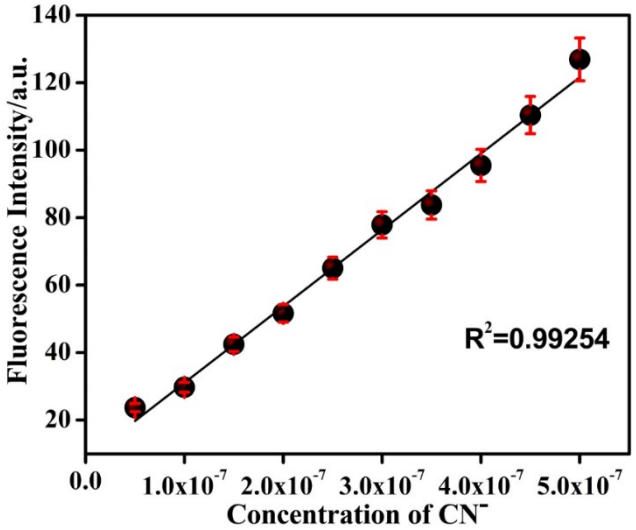

LOD Calculation

Formula = 3σ/slope

Standard deviation=0.45

Slope=2.26 X 10^8

LOD= 5.97 X10^{-9} or 5.97nM

Fig S6 Linear plot of **BID + CN^-**. The calculated limit of detection of 5.97 nM.

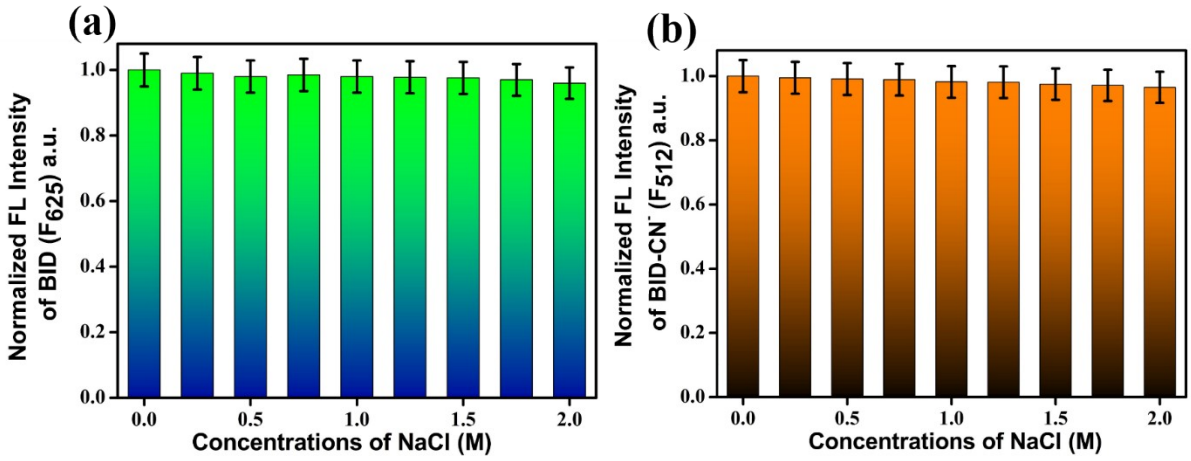

Fig S7 The effect of salt **(a, b)** on the normalized fluorescence intensity of **BID** and **BID+CN$^-$.**

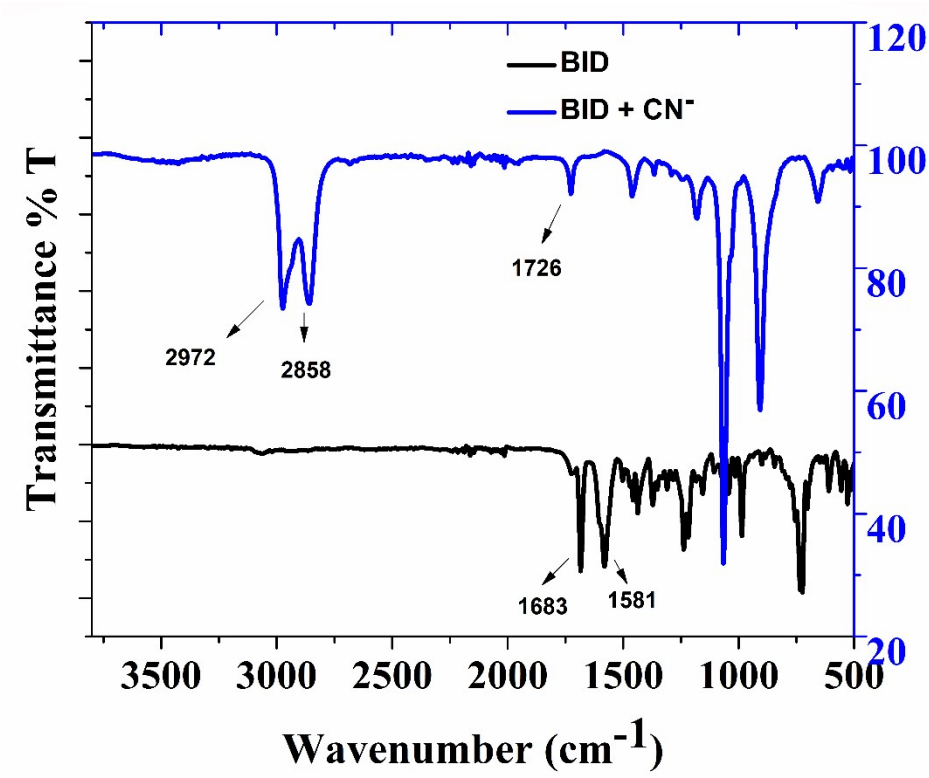

Fig S8 IR spectra of **BID** and **BID +CN$^-$.**

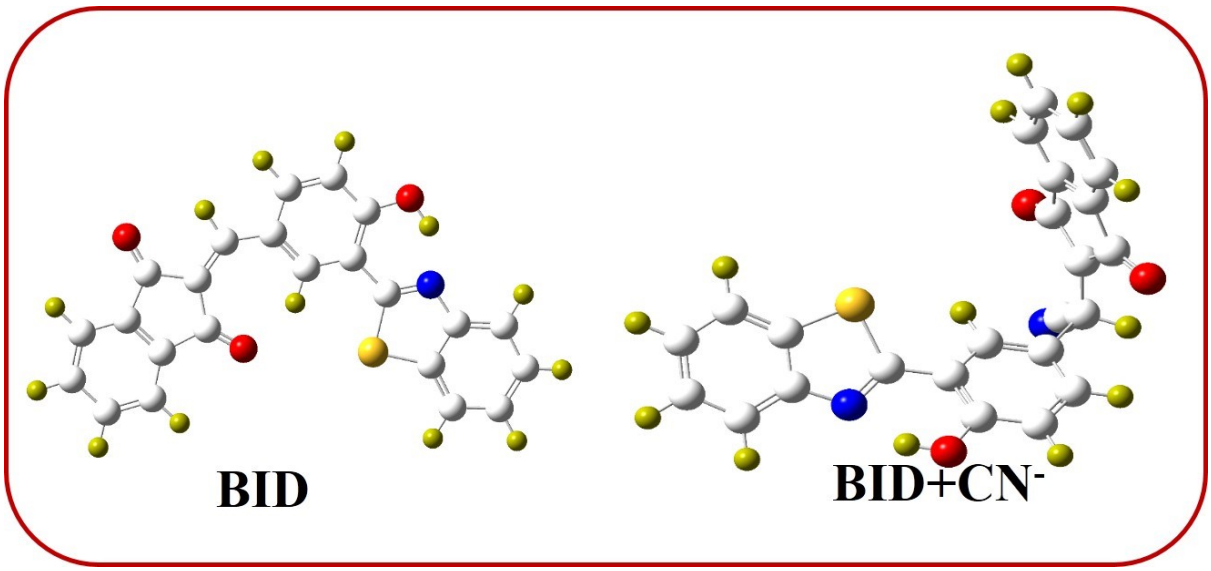

Fig S9 The entire geometry optimizations structure of **BID** and **BID+CN**$^-$ determined by DFT/B3LYP methods.

Table S1 Oscillator strengths of important transitions for the **BID** and **BID** + **CN**$^-$ determined by DFT/B3LYP methods.

Entry	λ max(nM)	Oscillatory strength	ΔE,Energy(eV)	Selected major transitions
	406.01	0.6990	18.5502	H ⟶ L (46%)
BID	369.07	0.0152	18.2996	H ⟶ L_1 (45%)
	358.11	0.3577	18.2275	H_1 ⟶ L (44%)
	334.77	0.3059	18.1976	H ⟶ L_2 (44%)
	293.94	0.3140	17.3404	H_2 ⟶ L_2 (40%)
	265.85	0.1932	7.8540	H ⟶ L_3 16%)
	298.45	0.0034	15.8748	H_4 ⟶ L (34%)
BID+ CN$^-$	345.19	0.0015	6.7614	H_3 ⟶ L_1 (12.3%)
	355.94	0.0005	3.5042	H ⟶ L (6.7%)
	355.94	0.0005	8.2374	H_2 ⟶ L (18.2%)
	360.29	0.0001	4.6482	H_1 ⟶ L_1 (11.6%)
	599.36	0.0076	2.7380	H_4 ⟶ L (4.1%)
	421.60	0.0005	2.9510	H_1 ⟶ L_4 (4.7%)
	415.73	0.0026	3.0509	H_5 ⟶ L_2 (5.0%)

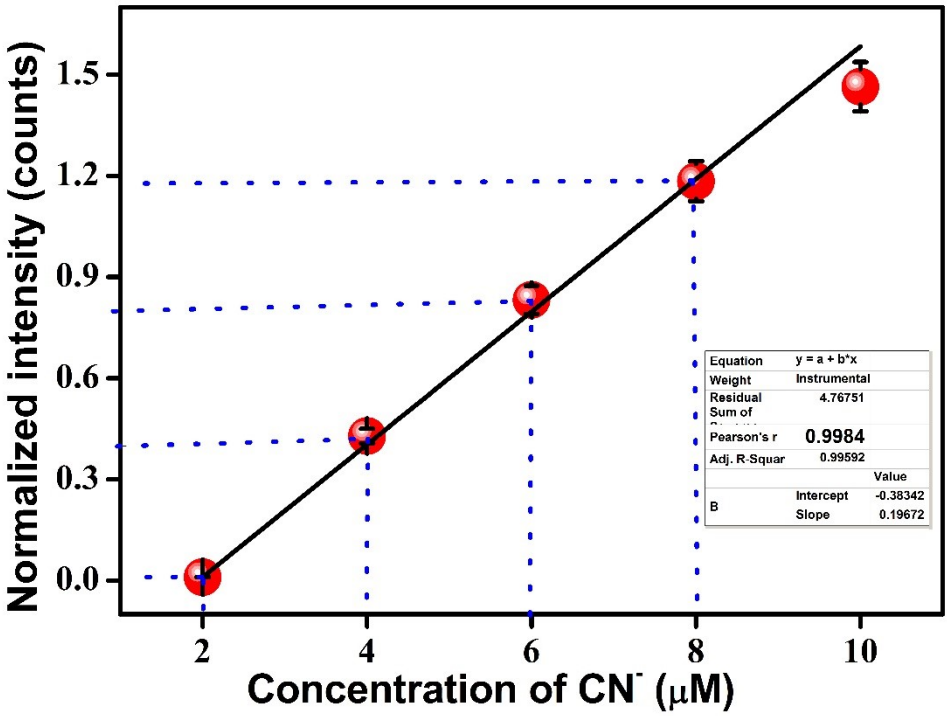

Fig S10 Quantitative calibration plot results for BID and incremental addition of CN^- (2-10 μM) for BID-CN^- samples in DMSO.

Table S2 Results of CN^- readings in DMSO samples.

Sample	Spiked (μM)	Found ($X^a \pm SD^b$) (μM)	Recovery (%)	RSD^c (%)
DMSO	2	1.979 ± 0.007	99.3	0.17
	4	3.988 ± 0.006	99.6	0.19
	6	6.013 ± 0.004	98.4	0.29

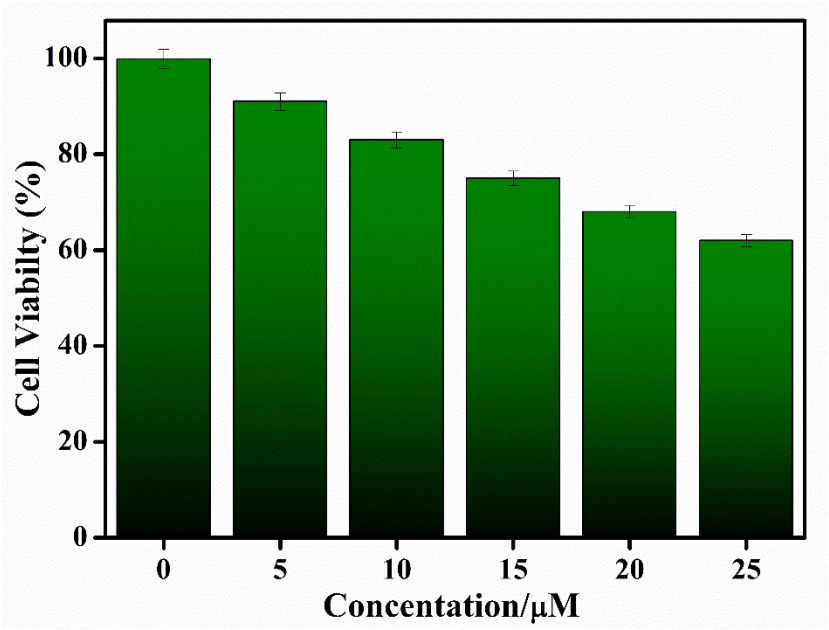

Fig S11 Cytotoxicity assay of sensor probe **BID**.

Table S3

Comparison of LOD of CN^- detection reported in recent papers.

S.No	Reported Probe	LOD	Reference
1	Naphthalimide based probes	1.7 μM	RSC Adv. 6 (2016) 33031-33035
2	Naphthylamide dye	7.7 μM	Scientific reports. 10 (2017) 41598-13325
3	Diethylaminosalicylaldehyde-Substituted based	3.39 μM	Dyes and Pigments. 174 (2019) 108049
4	Coumarin based sensor probe	2.07 μM	NJC. 43 (2019) 16796-16800.
5	(4-(2-(4-(diethylamino)phenyl)-4-methyl-5-oxo-4,5 dihydrothieno pyridin-7-yl)phenyl 2,4-dinitrobenzenesulfonate	3.2 μM	ACS OMEGA. 5 (2020) 32507−32514
6	Peptoid based	6.28 μM	ACS Applied Bio Materials. 3 (2020) 6039-6048
7	Naphthalene based sensor probe	1.1 μM	Chemcomm. 50 (2014) 12234
8	quinoline-indolium-based sensor probe	3.5 μM	NJC. 42 (2018) 5367–5375
9	Aminomalenonitrile based sensor probes	7.49 nM	Org. Biomol. Chem., 12 (2014) 479
10	Copper (II) complex ofazo-dye	2.5 μM	Spectrochimica Acta part A 10 (2017) 1016

11	Diketodiphenylpyrrolopyrrole	171 μM	Sensors Actuators B Chem. 245 (2017) 845–852
12	Indanedione based	9.4 μM	Sensors and Actuators B 233 (2016) 510–519
13	Phenylquinazolinone-based	40 μM	RSC Adv. 10 (2020) 44860–44875
14	Naphthoppyran based	7.56 μM	Spectrochimica Acta Part A: Molecular and Biomolecular Spectroscopy 217 (2019) 27–34
15	Disulfide Schiff base	250 μM	New J. Chem. 43 (2019) 13536–13544
16	Imidazole based	5.3 μM	Spectrochimica Acta Part A: Molecular and Biomolecular Spectroscopy 234 (2020) 118212
17	Azo salicylaldehyde based	1.95 μM	Inorganic Chemistry Communications 102 (2019) 83–89
18	1.3-indanedione based	1.7 μM	ACS Omega 2021, 6, 5287−5296
19	**benzothiazole-based**	**5.97nM**	**This work**